

- Suzuki A, Zheng YW, Kaneko S, Onodera M, Fukao K, Nakauchi H, Taniguchi H (2002) Clonal identification and characterization of self-renewing pluripotent stem cells in the developing liver. *The Journal of Cell Biology* 156, 173–184.
- Suzuki A, Iwama A, Miyashita H, Nakauchi H, Taniguchi H (2003) Role for growth factors and extracellular matrix in controlling differentiation of prospectively isolated hepatic stem cells. *Development* 130, 2513–2524.
- Suzuki T, Kanai Y, Hara T, Sasaki J, Sasaki T, Kohara M, Maehama T, Taya C, Shitara H, Yonekawa H, Frohman MA, Yokozeki T, Kanaho Y (2006) Crucial role of the small GTPase ARF6 in hepatic cord formation during liver development. *Molecular and Cellular Biology* 26, 6149–6156.
- Suzuki A, Sekiya S, Buscher D, Izpisua Belmonte JC, Taniguchi H (2008a) Tbx3 controls the fate of hepatic progenitor cells in liver development by suppressing p19ARF expression. *Development* 135, 1589–1595.
- Suzuki A, Sekiya S, Onishi M, Oshima N, Kiyonari H, Nakauchi H, Taniguchi H (2008b) Flow cytometric isolation and clonal identification of self-renewing bipotent hepatic progenitor cells in adult mouse liver. *Hepatology* 48, 1964–1978.
- Suzuki K, Tanaka M, Watanabe N, Saito S, Nonaka H, Miyajima A (2008c) p75 Neurotrophin receptor is a marker for precursors of stellate cells and portal fibroblasts in mouse fetal liver. *Gastroenterology* 135, 270–281 e273.
- Tanaka M, Hirabayashi Y, Sekiguchi T, Inoue T, Katsuki M, Miyajima A (2003) Targeted disruption of oncostatin M receptor results in altered hematopoiesis. *Blood* 102, 3154–3162.
- Tanaka M, Okabe M, Suzuki K, Kamiya Y, Tsukahara Y, Saito S, Miyajima A (2009) Mouse hepatoblasts at distinct developmental stages are characterized by expression of EpCAM and DLK1: drastic change of EpCAM expression during liver development. *Mechanisms of Development* 126, 665–676.
- Tang DQ, Lu S, Sun YP, Rodrigues E, Chou W, Yang C, Cao LZ, Chang LJ, Yang LJ (2006) Reprogramming liver-stem WB cells into functional insulin-producing cells by persistent expression of Pdx1- and Pdx1-VP16 mediated by lentiviral vectors. *Laboratory Investigation; A Journal of Technical Methods and Pathology* 86, 83–93.
- Tanimizu N, Miyajima A (2004) Notch signaling controls hepatoblast differentiation by altering the expression of liver-enriched transcription factors. *Journal of Cell Science* 117, 3165–3174.
- Tanimizu N, Miyajima A (2007) Molecular mechanism of liver development and regeneration. *International Review of Cytology* 259, 1–48.
- Tanimizu N, Tsujimura T, Takahide K, Kodama T, Nakamura K, Miyajima A (2004) Expression of Dlk/Pref-1 defines a subpopulation in the oval cell compartment of rat liver. *Gene Expr Patterns* 5, 209–218.
- Wang ND, Finegold MJ, Bradley A, Ou CN, Abdelsayed SV, Wilde MD, Taylor LR, Wilson DR, Darlington GJ (1995) Impaired energy homeostasis in C/EBP alpha knockout mice. *Science* 269, 1108–1112.
- Wang X, Foster M, Al-Dhalimy M, Lagasse E, Finegold M, Grompe M (2003) The origin and liver repopulating capacity of murine oval cells. *Proceedings of the National Academy of Sciences of the United States of America* 100 Suppl 1, 11881–11888.
- Wang AY, Ehrhardt A, Xu H, Kay MA (2007) Adenovirus transduction is required for the correction of diabetes using Pdx-1 or Neurogenin-3 in the liver. *Mol Ther* 15, 255–263.
- Watanabe T, Nakagawa K, Ohata S, Kitagawa D, Nishitai G, Seo J, Tanemura S, Shimizu N, Kishimoto H, Wada T, Aoki J, Arai H, Iwatsubo T, Mochita M, Watanabe T, Satake M, Ito Y, Matsuyama T, Mak TW, Penninger JM, Nishina H, Katada T (2002) SEK1/MKK4-mediated SAPK/JNK signaling participates in embryonic hepatoblast proliferation via a pathway different from NF-kappaB-induced anti-apoptosis. *Developmental Biology* 250, 332–347.
- Weinstein M, Monga SP, Liu Y, Brodie SG, Tang Y, Li C, Mishra L, Deng CX (2001) Smad proteins and hepatocyte growth factor control parallel regulatory pathways that converge on beta1-integrin to promote normal liver development. *Molecular and Cellular Biology* 21, 5122–5131.

- Yang L, Li S, Hatch H, Ahrens K, Cornelius JG, Petersen BE, Peck AB (2002) In vitro trans-differentiation of adult hepatic stem cells into pancreatic endocrine hormone-producing cells. *Proceedings of the National Academy of Sciences of the United States of America* 99, 8078–8083.
- Yang W, Yan HX, Chen L, Liu Q, He YQ, Yu LX, Zhang SH, Huang DD, Tang L, Kong XN, Chen C, Liu SQ, Wu MC, Wang HY (2008) Wnt/beta-catenin signaling contributes to activation of normal and tumorigenic liver progenitor cells. *Cancer Research* 68, 4287–4295.
- Yechool V, Liu V, Espiritu C, Paul A, Oka K, Kojima H, Chan L (2009) Neurogenin3 is sufficient for transdetermination of hepatic progenitor cells into neo-islets in vivo but not transdifferentiation of hepatocytes. *Developmental Cell* 16, 358–373.
- Yovchev MI, Grozdanov PN, Joseph B, Gupta S, Dabeva MD (2007) Novel hepatic progenitor cell surface markers in the adult rat liver. *Hepatology* 45, 139–149.
- Yovchev MI, Zhang J, Neufeld DS, Grozdanov PN, Dabeva MD (2009) Thymus cell antigen-1-expressing cells in the oval cell compartment. *Hepatology* 50, 601–611.
- Zajicek G, Oren R, Weinreb M, Jr. (1985) The streaming liver. *Liver* 5, 293–300.
- Zalzman M, Gupta S, Giri RK, Berkovich I, Sappal BS, Karnieli O, Zern MA, Fleischer N, Efrat S (2003) Reversal of hyperglycemia in mice by using human expandable insulin-producing cells differentiated from fetal liver progenitor cells. *Proceedings of the National Academy of Sciences of the United States of America* 100, 7253–7258.
- Zhao R, Duncan SA (2005) Embryonic development of the liver. *Hepatology* 41, 956–967.

## Retention in the Golgi apparatus and expression on the cell surface of Cfr/Esl-1/Glg-1/MG-160 are regulated by two distinct mechanisms

Yuichiro MIYAOKA<sup>\*1</sup>, Hidenori KATO<sup>\*1</sup>, Kazuki EBATO<sup>\*1</sup>, Shigeru SAITO<sup>\*</sup>, Naoko MIYATA<sup>\*</sup>, Toru IMAMURA<sup>†</sup> and Atsushi MIYAJIMA<sup>\*2</sup>

<sup>\*</sup>Laboratory of Cell Growth and Differentiation, Institute of Molecular and Cellular Biosciences, The University of Tokyo, Yayoi, Bunkyo-ku, Tokyo 113-0032, Japan, and <sup>†</sup>Signaling Molecules Research Group, Biomedical Research Institute, National Institute of Advanced Industrial Science and Technology (AIST), Tsukuba, Ibaraki 305-8566, Japan

Cfr (cysteine-rich fibroblast growth factor receptor) is an Fgf (fibroblast growth factor)-binding protein without a tyrosine kinase. We have shown previously that Cfr is involved in Fgf18 signalling via Fgf receptor 3c. However, as Cfr is also known as Glg (Golgi apparatus protein)-1 or MG-160 and occurs in the Golgi apparatus, it remains unknown how the distribution of Cfr is regulated. In the present study, we performed a mutagenic analysis of Cfr to show that two distinct regions contribute to its distribution and stability. First, the C-terminal region retains Cfr in the Golgi apparatus. Secondly, the Cfr repeats in the extracellular juxtamembrane region destabilizes Cfr passed through the Golgi apparatus. This destabilization does not depend on the cleavage and secretion of the extracellular domain of Cfr. Furthermore, we

found that Cfr with a GPI (glycosylphosphatidylinositol) anchor was predominantly expressed on the cell surface in Ba/F3 cells and affected Fgf18 signalling in a similar manner to the full-length Cfr, indicating that the interaction of Cfr with Fgfs on the cell surface is important for its function in Fgf signalling. These results suggest that the expression of Cfr in the Golgi apparatus and on the plasma membrane is finely tuned through two distinct mechanisms for exhibiting different functions.

**Key words:** cysteine-rich fibroblast growth factor receptor (Cfr), E-selectin ligand (Esl), fibroblast growth factor (Fgf), Golgi apparatus, mutagenesis.

### INTRODUCTION

Cfr (cysteine-rich fibroblast growth factor receptor) was identified originally as a transmembrane protein with affinity for Fgf (fibroblast growth factor) 1 and Fgf2 by biochemical screening [1]. It binds to Fgfs via a large extracellular domain comprising 16 repeats of a unique motif called the Cfr repeat, but has a short intracellular domain consisting of only 13 amino acid residues [2]. Cfr has no homology with known Fgf-binding molecules including Fgfrs (Fgf receptors) with a tyrosine kinase, and its physiological function had remained unknown. Recently, we generated *Cfr*-deficient mice, and found that they died in the perinatal period and show growth retardation and skeletal phenotypes. Because these phenotypes were similar to those of *Fgf18*-deficient mice, we examined the interaction between Cfr and Fgf18 biochemically and genetically, and demonstrated that Cfr binds to Fgf18 to positively regulate Fgf18 signalling through Fgfr3c [3].

However, Cfr is also known as Glg (Golgi apparatus protein)-1 or MG-160, and accumulating evidence indicates that it occurs predominantly in the Golgi apparatus in various cells [4–6]. Furthermore, Cfr has been shown to bind at least two other molecules, E-selectin and TGF $\beta$  (transforming growth factor  $\beta$ ), and is also known as Esl (E-selectin ligand)-1 and Ltbp (latent TGF $\beta$ -binding protein)-1 [7,8]. It was reported recently that Cfr binds to the TGF $\beta$  precursor in the Golgi apparatus to modify its maturation and secretion, regulating TGF $\beta$  function [9]. Because Cfr acts as an Fgf-binding protein, a ligand of E-selectin and a TGF $\beta$ -binding protein, its cellular position is critical for its function. To interact with extracellular cytokines Cfr must be on

the cell surface, but it can also interact with cytokines produced in the cell in the Golgi apparatus as reported for TGF $\beta$ . To bind E-selectin, Cfr must be on the cell surface. Thus Cfr is a unique multifunctional molecule and its intracellular distribution must be regulated.

Previous studies have suggested that the C-terminal cytoplasmic tail is important for the intracellular distribution of Cfr. Truncation of the cytoplasmic tail caused partial translocation of rat Cfr on to the cell surface in CHO (Chinese hamster ovary) cells [10]. Moreover, there exists an alternatively spliced variant of Cfr with an extension of 24 amino acid residues to the cytoplasmic tail in primates and humans. Human Cfr with or without the extension is located in the Golgi apparatus and on the cell surface respectively [11]. However, the involvement of other regions of Cfr in the regulation of its intracellular localization has not been examined.

To address this issue, we first confirmed that the cytoplasmic tail is important for the expression of Cfr in the Golgi apparatus, but noticed that without the tail the protein was extremely unstable. A GPI (glycosylphosphatidylinositol)-anchored Cfr mutant was directed to the cell surface and enhanced Fgf18 signalling via Fgfr3c, suggesting that Cfr positively regulates Fgf signalling on the cell surface rather than in the Golgi apparatus. However, it was also unstable and deletion mutants revealed that the Cfr repeats in the juxtamembrane domain contribute to the instability. Although it is known that Cfr is proteolytically cleaved at the juxtamembrane region and its extracellular domain is secreted [8,12], this cleavage is not involved in the instability. Furthermore, we demonstrated that the insertion of the Cfr repeats into the juxtamembrane region of EpCAM (epithelial cell-adhesion

Abbreviations used: Cfr, cysteine-rich fibroblast growth factor receptor; EGFP, enhanced green fluorescent protein; EpCAM, epithelial cell-adhesion molecule; Esl, E-selectin ligand; Fgf, fibroblast growth factor; Fgfr, Fgf receptor; Glg, Golgi apparatus protein; GPI, glycosylphosphatidylinositol; GST, glutathione transferase; IRES, internal ribosomal entry site; LFA, leucocyte function-associated antigen; TGF $\beta$ , transforming growth factor  $\beta$ ; Ltbp, latent TGF $\beta$ -binding protein; TGOLN2, *trans*-Golgi network protein 2; WST-1, water-soluble tetrazolium salt 1.

<sup>1</sup> These authors equally contributed to this work.

<sup>2</sup> To whom correspondence should be addressed (email miyajima@iam.u-tokyo.ac.jp).

molecule) also destabilized it, suggesting that the repeats are a module for protein destabilization. These results indicate that the intracellular distribution of Cfr is regulated by two distinct mechanisms. First, the transmembrane region and cytoplasmic tail retain Cfr in the Golgi apparatus, and secondly the extracellular juxtamembrane Cfr repeats destabilize Cfr passed through the Golgi apparatus, allowing Cfr to exhibit its unique multiple functions.

## MATERIALS AND METHODS

### cDNAs

In all of the mutants of Cfr used in the present study, the signal sequence of mouse Cfr (amino acids 1–27) was replaced by the signal sequence of mouse CD2 and a FLAG tag. FLAG–Cfr $\Delta$ 1169, corresponding to the reported rat  $\Delta$ 1165 mutant [10], was generated by deleting the C-terminal six amino acid residues (RELKDR). In all of the GPI-anchored mutants, the extracellular domain of Cfr (amino acids 1–1141) was fused to the signal sequence for the GPI-anchor of human CD58 [also known as LFA (leucocyte function-associated antigen) 3, amino acids 204–237] [13]. In FLAG–Cfr–KARA–GPI, KR (amino acids 1096–1097) and KKR (amino acids 1105–1107) were replaced with AA and AAA respectively. In FLAG–Cfr $\Delta$ 13–16–GPI and FLAG–Cfr $\Delta$ 13–16, Cfr repeats 13–16 (amino acids 870–1141) were deleted. Similarly, in FLAG–Cfr $\Delta$ 15–16–GPI and FLAG–Cfr $\Delta$ 16–GPI, repeats 15 and 16 (amino acids 995–1141) and repeat 16 (amino acids 1057–1141) were deleted. In EpCAM–CfrRepeat, Cfr repeats 13–16 were inserted between the C-terminus of the extracellular domain and the N-terminus of the transmembrane region of mouse EpCAM (between amino acids 266 and 267).

### Antibodies

The antibodies used were as follows: anti-FLAG M2 antibody (F3165) from Sigma, anti-actin antibody (sc-1616) from Santa Cruz Biotechnology, anti-TGOLN2 (*trans*-Golgi network protein 2, also known as Tgn38 and Tgn46) antibody (ab16059) and anti-EpCAM antibody (for Western blot analysis) (ab32392) from Abcam, and anti-EpCAM antibody (for immunofluorescent staining) (552370) from BD Pharmingen. The rabbit serum against Cfr and a rat monoclonal antibody against EpCAM (for flow cytometry) have been described previously [3,14].

### Inhibition of lysosomes and proteasomes

Ba/F3 cells were incubated in medium containing 10 mM NH<sub>4</sub>Cl (Wako) as a lysosomal enzyme inhibitor, or 10 mM MG-132 (Sigma) as a proteasome inhibitor at 37 °C for 12 h. In parallel with these treatments, Ba/F3 cells were also incubated in medium with PBS and DMSO as a control. The cells were then either harvested for Western blot analysis or analysed by flow cytometry for cell-surface expression of the FLAG-tagged Cfr proteins.

### Retroviral infection and proliferation of Ba/F3 cells

Ba/F3 cells and NIH 3T3 cells were infected with retroviruses containing cDNA for a Cfr mutant with an IRES (internal ribosomal entry site)–EGFP (enhanced green fluorescent protein) sequence. The methods used for the proliferation assay have been described previously [3]. Briefly, we sorted EGFP-positive Ba/F3 cells by FACS Vantage (BD), and performed the assay in 96-well plates with WST-1 (water-soluble tetrazolium salt 1; Roche

Applied Science). GST (glutathione transferase) and GST–Fgf18 used in the present study were described previously [3].

### Protein stability assay

Ba/F3 cells were incubated with 50  $\mu$ g/ml cycloheximide for different periods of time and then harvested for Western blot analysis.

### Immunofluorescent staining

Ba/F3 cells were fixed with 4 % paraformaldehyde in PBS at room temperature (25 °C) for 10 min. The cells were incubated with primary antibodies in 5 % skimmed milk in PBS at 4 °C overnight. They were then incubated with secondary antibodies in 5 % skimmed milk in PBS at room temperature for 2 h, and embedded in GEL/MOUNT (Biomedica) containing Hoechst 33342. Signals were observed under a confocal microscope.

### Biotin-labelling assay

Ba/F3 cells were washed three times with ice-cold PBS with 0.7 mM CaCl<sub>2</sub> and 0.5 mM MgCl<sub>2</sub>. Biotinylation of cell-surface proteins was performed with 500  $\mu$ l of 300  $\mu$ g/ml EZ-Link-Sulfo-NHS-SS-biotin (Pierce) in PBS for 30 min at 4 °C. Unbound biotin was removed by three washes with ice-cold PBS. Biotinylated cells were incubated with 500  $\mu$ l of lysis buffer [50 mM Tris/HCl (pH 7.5), 150 mM NaCl, 1 % Nonidet P40, 1 mM EDTA, 1  $\mu$ g/ml leupeptin (Roche Applied Science), 1 mM PMSF (Wako) and 500  $\mu$ g/ml Pefabloc (Roche Applied Science)] for 1 h at 4 °C. Immuno-Pure immobilized streptavidin (Pierce) was then added to biotinylated cell lysate and incubated for 2 h at 4 °C to pull down the biotin-labelled proteins. After washing three times with the lysis buffer, the resins were boiled and the pulled down proteins were subjected to Western blot analysis.

### Western and Northern blot analyses

The methods used for the Western and Northern blot analyses have been described previously [15].

## RESULTS

### Intracellular distribution of Cfr in Ba/F3 cells

We reported previously that forced expression of Cfr enhanced Fgf18 signalling via Fgfr3c in Ba/F3 cells [3]. Cfr, however, has been known as a protein of the Golgi apparatus, so we investigated the intracellular distribution of Cfr by expressing the protein with a FLAG tag at its N-terminus (FLAG–Cfr) in Ba/F3 cells (Figure 1A). Flow cytometric analysis with an anti-FLAG antibody showed that FLAG–Cfr was significantly expressed on the cell surface (Figure 1B). By contrast, immunofluorescent microscopic observation with the anti-FLAG antibody revealed that FLAG–Cfr occurred predominantly in the Golgi apparatus, whereas its expression on the cell surface was barely detectable (Figure 1C).

### Cfr lacking the cytoplasmic tail enhances Fgf18 signalling on the cell surface

Because FLAG–Cfr was located both on the cell surface and in the Golgi apparatus, it was not clear where Cfr functions in Fgf18 signalling. Therefore we attempted to restrict Cfr to the

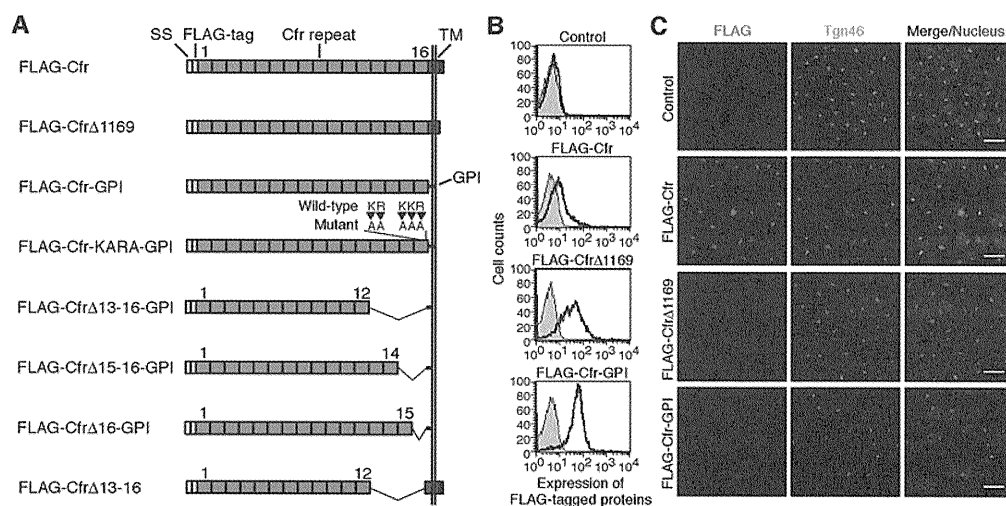


**Figure 1** Intracellular distribution of the C-terminally modified Cfr mutants in Ba/F3 cells

(A) Schematic representation of the Cfr mutants. All of the mutant proteins have a FLAG tag at their N-terminus. The GPI-anchored mutants have a GPI signal sequence by which they are recruited to the cell surface via GPI. Deleted regions and point-mutated sites are also indicated. SS, signal sequence; TM, transmembrane domain. (B) Expression of FLAG-Cfr, FLAG-Cfr $\Delta$ 1169 and FLAG-Cfr-GPI on the Ba/F3 cell surface monitored by flow cytometry. Ba/F3 cells with only EGFP were used as a control. Note that FLAG-Cfr was significantly expressed on the cell surface compared with the control cells, and the C-terminal modification enhanced the surface expression. The filled plot is the isotype control and open plot is the anti-FLAG. (C) Immunofluorescent staining of FLAG (red) in Ba/F3 cells. The Golgi apparatus was also visualized by staining of TGOLN2 (Tgn46, green). In the merged photographs, signals of FLAG, TGOLN2 and nuclei (blue) are merged. Scale bar, 20  $\mu$ m.

cell surface. For this purpose, we generated two Cfr mutants by modifying the C-terminal domain, as it was reported that the C-terminal cytoplasmic region is required for the expression of Cfr in the Golgi apparatus [10]. One mutant was a FLAG-tagged Cfr without the C-terminal cytoplasmic tail (FLAG-Cfr $\Delta$ 1169), which corresponds to the rat Cfr mutant reported to be expressed on the cell surface [10] (Figure 1A). The other comprised the FLAG-tagged extracellular domain of Cfr fused to the well-characterized GPI signal peptide of human CD58 [13] (FLAG-Cfr-GPI) (Figure 1A). We expressed these two mutants in Ba/F3 cells, and monitored their intracellular distribution. As expected, the surface expression of these mutants was stronger than that of FLAG-Cfr, and they were barely detected in the Golgi apparatus (Figures 1B and 1C).

We then established Ba/F3 cells expressing Fgfr3c with either FLAG-Cfr or FLAG-Cfr-GPI to determine their response to Fgf18. Consistent with our previous report, FLAG-Cfr enhanced Fgf18 signalling via Fgfr3c in Ba/F3 cells (Figure 2). Furthermore, Ba/F3 cells with FLAG-Cfr-GPI, like those with FLAG-Cfr, more strongly responded to Fgf18 than control cells (Figure 2). These results suggest that the positive effect of Cfr on Fgf signalling is determined by its level of expression on the cell surface, not in the Golgi apparatus. Furthermore, the cytoplasmic tail is unnecessary for the function of Cfr in Fgf signalling.

#### Instability of the C-terminally modified Cfr mutants

As Cfr expressed on the cell surface enhances Fgf18 signalling, the regulation of its transport from the Golgi apparatus to the cell surface is important for its functions. Therefore we investigated further the regulatory mechanisms governing the intracellular distribution of Cfr.

We noticed that the cell-surface expression of the C-terminally modified mutants FLAG-Cfr $\Delta$ 1169 and FLAG-Cfr-GPI was rather weak and that it was under the detection limit of the biotin-labelling assay (Figure 1B and results not shown). Therefore we checked mRNA and protein levels and found that the amount of

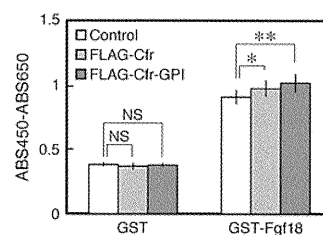


**Figure 2** Effects of FLAG-Cfr-GPI on Fgf18 signalling

Ba/F3 cells expressing both Fgfr3c and FLAG-Cfr-GPI, as well as those with Fgfr3c and FLAG-Cfr were stimulated with 500 ng/ml GST (glutathione transferase)-Fgf18. The same amount of GST was added as a control. The extent of proliferation was monitored by WST-1 assay, and absorbance at 450 nm minus basal absorbance at 650 nm  $\pm$  S.D. is shown. We prepared eight wells for each condition. FLAG-Cfr-GPI enhanced Fgf18 signalling like FLAG-Cfr. *P* value was calculated with Student's *t* test: \* *P* < 0.05; \*\* *P* < 0.01; NS, *P* > 0.2.

protein was greatly reduced for FLAG-Cfr $\Delta$ 1169 and FLAG-Cfr-GPI compared with FLAG-Cfr, whereas the amount of mRNA was comparable with that for FLAG-Cfr (Figure 3A). The results indicate that these mutant proteins are unstable, raising the possibility that lysosomal or proteasomal degradation may occur. To address this possibility, a lysosomal enzyme inhibitor NH<sub>4</sub>Cl or a proteasome inhibitor MG-132 were added to the cells. However, neither inhibitor rescued the total amount of FLAG-Cfr-GPI protein (Figure 3B). Moreover, these inhibitors failed to recover the cell-surface expression of FLAG-Cfr-GPI (Figure 3C). The results suggest that these Cfr mutants were destabilized by another mechanism.

#### Shedding of Cfr is not involved in the instability of the Cfr mutants

Because previous reports have shown that the extracellular domain of Cfr is cleaved in the juxtamembrane region to be secreted into the culture supernatant [8,12], we considered the possibility that the instability of Cfr is caused by shedding rather than degradation through the lysosome or proteasome. Therefore

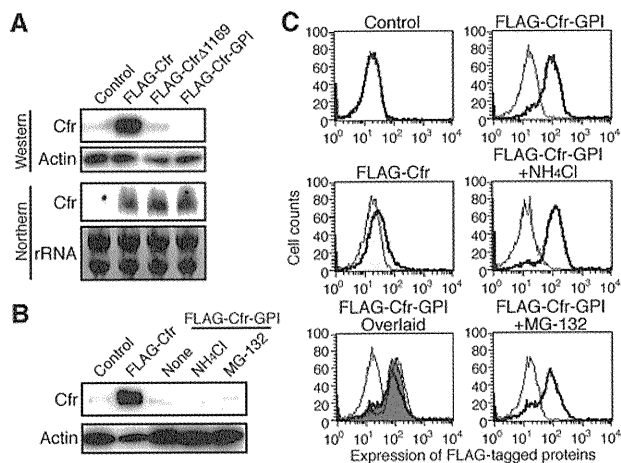


**Figure 3** Protein and mRNA expression of the C-terminally modified mutants in Ba/F3 cells

(A) Western and Northern blot analyses of protein and mRNA expression of the C-terminal mutants in Ba/F3 cells. The total amount of protein and RNA loaded was monitored by blotting with an anti-actin antibody and visualization of rRNA with ethidium bromide respectively. The protein expression of the mutants is dramatically reduced compared with that of FLAG-Cfr, whereas the mRNA levels are comparable. Note that the endogenous full-length Cfr was also detected in all samples with anti-Cfr serum. (B) Effect of inhibitors for lysosomal enzymes or proteasomes on protein expression of FLAG-Cfr-GPI in Ba/F3 cells. Ba/F3 cells expressing FLAG-Cfr-GPI were incubated with a lysosomal enzyme inhibitor ( $\text{NH}_4\text{Cl}$ ), a proteasome inhibitor (MG-132) or solvent (None) for 12 h. (C) Effect of  $\text{NH}_4\text{Cl}$  and MG-132 on the cell-surface expression of FLAG-Cfr-GPI. The cell-surface expression of FLAG-Cfr-GPI in Ba/F3 cells treated with  $\text{NH}_4\text{Cl}$  and MG-132 was analysed by flow cytometry. For each sample: filled, isotype controls; open, anti-FLAG. For the lower left-hand panel: filled, isotype control of None (light grey), anti-FLAG of None (dark grey) and overlaid,  $\text{NH}_4\text{Cl}$  (thin line), and MG-132 (bold line). Neither inhibitor recovered the protein expression of FLAG-Cfr-GPI.

we investigated the amount of the shed extracellular domain of Cfr in the culture supernatants of Ba/F3 cells expressing FLAG-Cfr or FLAG-Cfr-GPI. We immunoprecipitated the extracellular domain from the culture supernatants by the anti-FLAG antibody. As shown in Figure 4(A), the amounts of proteins precipitated were comparable between FLAG-Cfr and FLAG-Cfr-GPI, whereas the amount of FLAG-Cfr-GPI in the cell lysate was extremely low compared with that of FLAG-Cfr, indicating that the shedding of the extracellular domain was not a main cause of the instability. As there are two potential basic proteolytic cleavage sites in the juxtamembrane region of Cfr [8], we investigated further the involvement of shedding in the protein instability by introducing point mutations into FLAG-Cfr-GPI to replace the basic sites KR and KKR with an alanine residue (FLAG-Cfr-KARA-GPI) (Figure 1A). We expressed the mutant in Ba/F3 cells and monitored its expression. Flow cytometric analysis showed that there was no difference in cell-surface expression between FLAG-Cfr-GPI and FLAG-Cfr-KARA-GPI (Figure 4B). Although Northern blot analysis showed that the mRNA levels of FLAG-Cfr-KARA-GPI and FLAG-Cfr-GPI were comparable, and greater than that of FLAG-Cfr, the protein levels were not increased by the mutation (Figure 4C). These results clearly indicate that proteolytic cleavage in the juxtamembrane region is not involved in the instability of the Cfr mutants with the C-terminal modification.

#### Cfr repeats in the juxtamembrane region destabilize Cfr

Because the basic amino acid sites in the juxtamembrane region do not appear to destabilize Cfr, we examined a possibility that the stability of Cfr is regulated by the Cfr repeats. For this

purpose we generated deletion mutants. As shown in Figure 1(A), the extracellular domain of Cfr is composed of 16 repeats of a unique motif, the Cfr repeat. First, we deleted repeats 13–16 from FLAG-Cfr-GPI (FLAG-Cfr $\Delta$ 13–16-GPI) (Figure 1A), and expressed the mutant in Ba/F3 cells. Surprisingly, FLAG-Cfr $\Delta$ 13–16-GPI was expressed more strongly on the cell surface than FLAG-Cfr-GPI, and FLAG-Cfr $\Delta$ 13–16-GPI was clearly detected by Western blotting unlike FLAG-Cfr-GPI (Figures 4A, 5A and 5B). Therefore the deleted juxtamembrane domain is critical for the stability of Cfr. To narrow down the region, we generated two additional mutants FLAG-Cfr $\Delta$ 15–16-GPI and FLAG-Cfr $\Delta$ 16-GPI in which the last two repeats and last repeat were deleted from FLAG-Cfr-GPI respectively (Figure 1A), and expressed them in Ba/F3 cells. Unexpectedly, FLAG-Cfr $\Delta$ 15–16-GPI and FLAG-Cfr $\Delta$ 16-GPI were expressed on the cell surface at levels in between those of FLAG-Cfr-GPI and FLAG-Cfr $\Delta$ 13–16-GPI (Figure 5A). Overlaying the flow cytometric profiles clearly showed that the GPI-anchored mutants with fewer Cfr repeats exhibited stronger expression on the cell surface (Figure 5A). We also detected FLAG-Cfr $\Delta$ 15–16-GPI and FLAG-Cfr $\Delta$ 16-GPI by Western blotting, indicating that these mutants were more stable than FLAG-Cfr-GPI (Figure 5B). Furthermore, immunofluorescent staining revealed increased cell-surface expression of FLAG-Cfr $\Delta$ 13–16-GPI compared with FLAG-Cfr-GPI (Figure 5C). On the basis of these results, we concluded that without the C-terminal domain, more Cfr is recruited to the cell surface from the Golgi apparatus, but the juxtamembrane Cfr repeats destabilize the Cfr protein, reducing its cell-surface expression.

#### Cfr protein is unstable outside the Golgi apparatus

To investigate the instability of Cfr protein more directly, we determined the half-lives of the Cfr mutants. For this purpose, we added cycloheximide to Ba/F3 cells expressing the Cfr mutants and monitored their amounts by Western blot analysis. The full-length Cfr was stable and the protein level was not changed significantly, even after 5 h in this assay (Figure 6A). By contrast, the protein level of FLAG-Cfr-GPI was too low to determine the half-life in this assay (Figures 3A and 3B, and results not shown). Therefore we determined the half-lives of the Cfr mutants with intermediate stability, FLAG-Cfr $\Delta$ 13–16-GPI and FLAG-Cfr $\Delta$ 15–16-GPI. In contrast with the full-length Cfr, these mutants were unstable and their amounts declined by the addition of cycloheximide (Figure 6A). On the basis of three independent experiments, the half-lives of FLAG-Cfr $\Delta$ 13–16-GPI and FLAG-Cfr $\Delta$ 15–16-GPI were estimated to be 102.6 and 92.7 min respectively (Figure 6B). These results clearly show that Cfr is stable in the Golgi apparatus, whereas it is highly unstable outside the Golgi apparatus.

#### Retention of Cfr in the Golgi apparatus through its C-terminus prior to destabilization by the Cfr repeats

We then deleted the Cfr repeats 13–16 from FLAG-Cfr (FLAG-Cfr $\Delta$ 13–16) (Figure 1A), and expressed the mutant in Ba/F3 cells. The level of FLAG-Cfr $\Delta$ 13–16 on the cell surface was comparable with that of FLAG-Cfr in the flow cytometric analysis (Figure 7A). Western blot analysis revealed that the amount of protein was also comparable with that of FLAG-Cfr, and robustly increased compared with that of FLAG-Cfr $\Delta$ 13–16-GPI (Figure 7B). Moreover, we observed that FLAG-Cfr $\Delta$ 13–16 was mostly present in the Golgi apparatus like FLAG-Cfr,

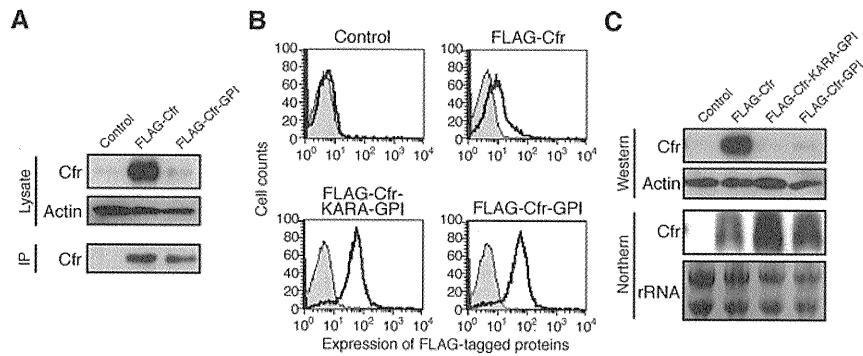


**Figure 4** Expression of the Cfr with mutations in the juxtamembrane basic sites

(A) Secretion of the extracellular domain of Cfr into the culture supernatants of Ba/F3 cells. The extracellular domain was immunoprecipitated from the culture supernatants of Ba/F3 cells expressing FLAG-Cfr or FLAG-Cfr-GPI, and then subjected to Western blot analysis (IP). Expression of Cfr in Ba/F3 cells and the total amount of the cell lysate loaded was monitored by blotting with anti-Cfr serum and anti-actin antibody respectively (Lysate). The amount of the extracellular domain secreted was comparable between FLAG-Cfr and FLAG-Cfr-GPI. (B) Cell-surface expression of FLAG-Cfr-KARA-GPI. Filled, isotype control; open, anti-FLAG. No difference in the expression level was observed between FLAG-Cfr-KARA-GPI and FLAG-Cfr-GPI. (C) The total amount of FLAG-Cfr-KARA-GPI protein and mRNA in Ba/F3 cells. Mutations in the two basic sites did not alter the amount of total protein expression from FLAG-Cfr-GPI.

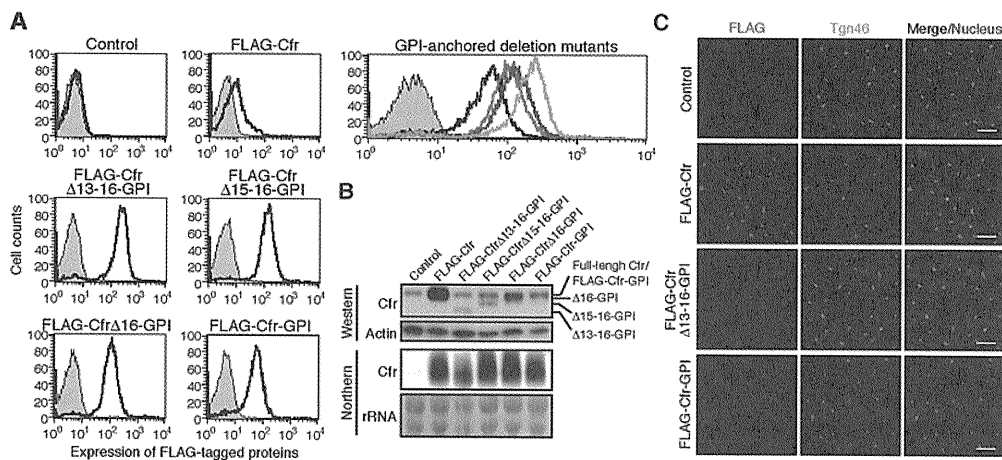


**Figure 5** Expression of the mutants deleted of the Cfr repeats in Ba/F3 cells

(A) Flow cytometric analysis of the GPI-anchored deletion mutants. Cell-surface expression of the mutants was monitored using the FLAG tag. For each sample: filled, isotype control; open, anti-FLAG. For the panel showing GPI-anchored deletion mutants: filled, isotype control of FLAG-Cfr-GPI; overlaid, anti-FLAG of FLAG-Cfr-GPI (black), FLAG-Cfr  $\Delta$ 16-GPI (red), FLAG-Cfr  $\Delta$ 15-16-GPI (blue) and FLAG-Cfr  $\Delta$ 13-16-GPI (green). Cell-surface expression of the GPI-anchored Cfr mutants increased as the number of Cfr repeats decreased. (B) Western and Northern blot analyses of total protein and mRNA of the deletion mutants. The mutants were clearly detected in the Western blot analysis. (C) Immunofluorescent staining of Ba/F3 cells expressing the deletion mutants. In the merged photographs, signals of FLAG (red), TGOLN2 (Tgn46, green) and nuclei (blue) are merged. Scale bar, 20  $\mu$ m. The FLAG signals on the cell surface were slightly stronger in FLAG-Cfr  $\Delta$ 13-16-GPI than FLAG-Cfr-GPI.

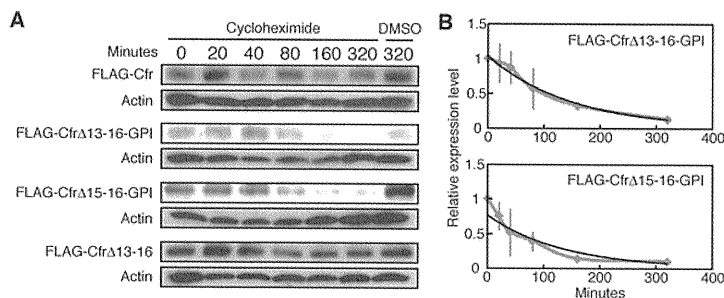


**Figure 6** Protein stability assay of the Cfr mutants

(A) Ba/F3 cells expressing the Cfr mutants were incubated with 50  $\mu$ g/ml cycloheximide for the indicated periods, and then harvested for Western blot analysis. As a control the solvent DMSO was added. The GPI-anchored mutants showed decreased stability. By contrast, FLAG-Cfr and FLAG-Cfr  $\Delta$ 13-16 was stable and showed no decline in the amount of protein. (B) The half-life curves for the GPI-anchored mutants. The half-lives of FLAG-Cfr  $\Delta$ 13-16-GPI and FLAG-Cfr  $\Delta$ 15-16-GPI are 102.6 and 92.7 min respectively.

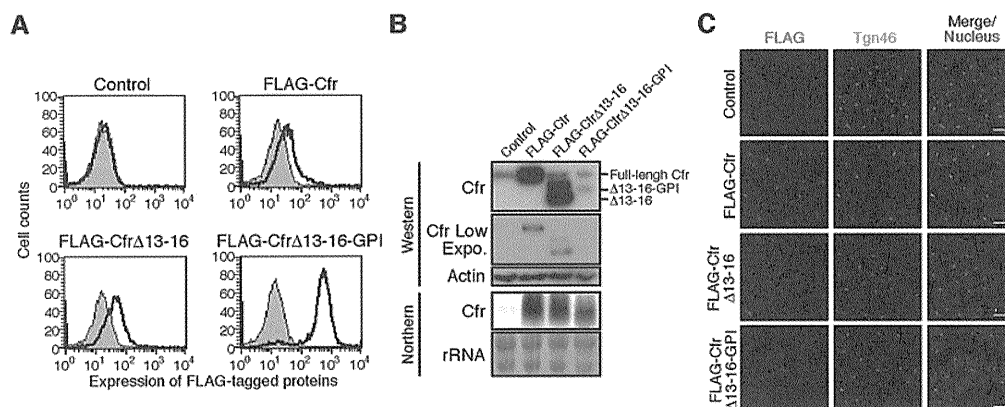


**Figure 7** Retention of the Cfr deletion mutant in the Golgi apparatus by the C-terminus of Cfr

(A) Flow cytometric analysis of FLAG-CfrΔ13-16. Filled, isotype control; open, anti-FLAG. Deletion of the Cfr repeats did not strongly enhance the cell-surface expression of FLAG-Cfr in the presence of the transmembrane domain and cytoplasmic tail. (B) Western and Northern blot analyses of FLAG-CfrΔ13-16 protein and mRNA. The results of low exposure in the Western blot analysis are also shown (Cfr Low Expo.). The amounts of FLAG-Cfr and FLAG-CfrΔ13-16 are comparable. (C) Immunofluorescent staining of FLAG-CfrΔ13-16 in Ba/F3 cells. In the merged panels, signals of FLAG (red), TGOLN2 (Tgn46, green) and nuclei (blue) are merged. Scale bar, 20 μm. Unlike FLAG-CfrΔ13-16-GPI, FLAG-CfrΔ13-16 was mostly located in the Golgi apparatus.

**Table 1** Summary of intracellular distribution and protein stability of the Cfr mutants

Comparison with FLAG-Cfr-GPI are shown for some of the mutants.

Cfr mutant	Intracellular distribution	Protein stability
FLAG-Cfr	Golgi and weakly cell surface	Very stable
FLAG-CfrΔ1169	Cell surface	Unstable
FLAG-Cfr-GPI	Cell surface	Unstable
FLAG-CfrΔ13-16-GPI	Cell surface (>FLAG-Cfr-GPI)	Stable (>FLAG-Cfr-GPI)
FLAG-CfrΔ15-16-GPI	Cell surface (>FLAG-Cfr-GPI)	Stable (>FLAG-Cfr-GPI)
FLAG-CfrΔ16-GPI	Cell surface (>FLAG-Cfr-GPI)	Stable (>FLAG-Cfr-GPI)
FLAG-Cfr-KARA-GPI	Cell surface (= FLAG-Cfr-GPI)	Unstable (= FLAG-Cfr-GPI)
FLAG-CfrΔ16	Golgi and weakly cell surface	Very stable

indicating that destabilization of Cfr by the Cfr repeats does not occur in the Golgi apparatus (Figure 7C). This possibility was further supported by the stability of FLAG-CfrΔ13-16, which was comparable with that of the full-length Cfr (Figure 6A).

#### Regulatory mechanisms for the intracellular distribution of Cfr in other cells and proteins

Finally, we addressed whether the regulatory mechanisms for the intracellular distribution of Cfr are general. First, we expressed the Cfr mutants in NIH 3T3 cells to confirm our results in Ba/F3 cells, and found that the mutants were expressed in NIH 3T3 cells with patterns basically the same as those in Ba/F3 cells (Figure 8A). In addition, we also observed that the Cfr mutants were expressed with the same patterns in COS7 cells (results not shown). We have summarized the intracellular distribution and protein stability of the Cfr mutants in Table 1.

Next, we investigated whether the mechanisms work in other proteins. It has been already shown that fusion of the C-terminal region of Cfr to the extracellular domain of CD8 directs the fusion protein to the Golgi apparatus [11]. Therefore we generated a fusion protein of another cell-surface protein EpCAM and the Cfr repeats (EpCAM-CfrRepeat; Figure 8B). We expressed this fusion protein in Ba/F3 cells in parallel with wild-type EpCAM, and monitored their expression on the cell surface by flow cytometry and a biotin-labelling assay. Interestingly, the insertion of the Cfr

repeats decreased the surface expression of EpCAM (Figures 8C and 8D). We then monitored mRNA and protein expression of EpCAM-CfrRepeat and found that whereas the amount of mRNA was comparable between EpCAM and EpCAM-CfrRepeat, the amount of EpCAM-CfrRepeat protein was extremely low (Figure 8E). We monitored further the intracellular distribution of EpCAM-CfrRepeat by immunofluorescent staining. EpCAM was expressed strongly on the cell surface, but the strength of the EpCAM-CfrRepeat signal was lower than that of EpCAM (Figure 8F).

These results clearly show that Cfr is at first retained in the Golgi apparatus through its transmembrane domain and cytoplasmic tail, and then subjected to stability control through the Cfr repeats during its recruitment to the plasma membrane or on the cell surface (Figure 8G).

#### DISCUSSION

Cfr is unique in that it has been identified independently as an Fgf-binding protein, a latent TGFβ-binding protein, a ligand for E-selectin and a protein of the Golgi apparatus [1,4,7,8]. However, its physiological functions had been unknown. Recently, we [3] and Yang et al. [9] independently generated *Cfr*-deficient mice and reported that they show skeletal phenotypes. We reported that Cfr is a positive regulator of the Fgf18 signalling pathway, and revealed in the present study that the interaction between Cfr and Fgf18 on the cell surface is important for Cfr's actions (Figure 2), whereas Yang et al. [9] indicated that it also contributes to TGFβ signalling by binding the precursor of TGFβ in the Golgi apparatus. Furthermore, the function of Cfr as a ligand for E-selectin has been well confirmed by knockdown experiments, although no obvious phenotype in cell adhesion via selectins, such as lymphocyte rolling, has been observed in *Cfr*-deficient mice [16]. Cfr is ubiquitously expressed in almost all cells and tissues from very early in embryonic development to adulthood [3]. Therefore, considering the pleiotropic roles of Fgf and TGFβ signalling in development, the phenotypes of *Cfr*-deficient mice would be much more severe if Cfr functions the same way in all cells. Rather, Cfr seems to perform different roles according to its cellular context. We speculate that a key determinant is its intracellular distribution. When located in the Golgi apparatus,



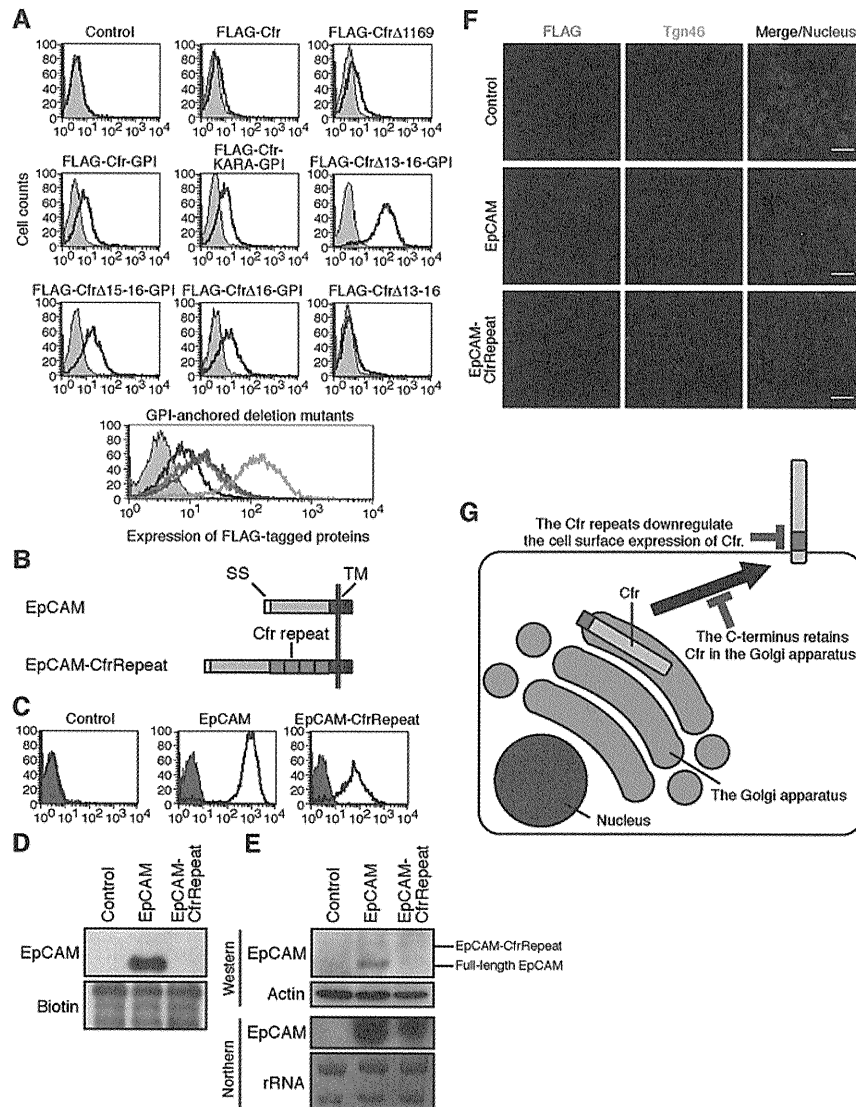


**Figure 8** Cell-surface expression of the Cfr mutants in NIH 3T3 cells and destabilization of EpCAM by the Cfr repeats

(A) Flow cytometric analysis of the cell-surface expression of the Cfr mutants in NIH 3T3 cells. For each sample: filled, isotype control; open, anti-FLAG. For the panel showing GPI-anchored deletion mutants: filled, isotype control of FLAG-Cfr-GPI; open, anti-FLAG of FLAG-Cfr-GPI (black), FLAG-Cfr $\Delta$ 16-GPI (red), FLAG-Cfr $\Delta$ 15-16-GPI (blue) and FLAG-Cfr $\Delta$ 13-16-GPI (green). (B) Schematic representation of EpCAM-CfrRepeat. EpCAM-CfrRepeat has Cfr repeats 13-16 inserted between the extracellular domain and transmembrane region of EpCAM. SS, signal sequence; TM, transmembrane domain. (C) Cell-surface expression of EpCAM and EpCAM-CfrRepeat monitored by biotin labelling assay. Filled, isotype control; open, anti-EpCAM. (D) Cell surface expression of EpCAM and EpCAM-CfrRepeat monitored by biotin labelling assay. Proteins on the cell surface were biotin-labelled and pulled down. The precipitates were subjected to Western blot analysis for EpCAM. The total amount of biotin-labelled surface protein was monitored by streptavidin (biotin). (E) Western and Northern blot analyses of EpCAM and EpCAM-CfrRepeat protein and mRNA. (F) Immunofluorescent staining of EpCAM and EpCAM-CfrRepeat in Ba/F3 cells. In the merged panels, signals of EpCAM (red), TGN2 (Tgn46, green) and nuclei (blue) are merged. Scale bar, 20  $\mu$ m. (G) A two-step model for regulation of the intracellular distribution of Cfr. First, Cfr is subjected to selection between retention in the Golgi apparatus and transport to the cell surface. The C-terminus of Cfr is involved in this process to retain Cfr in the Golgi apparatus. Secondly, the amount of Cfr on the cell surface is controlled by its stability. With the Cfr repeats, Cfr is destabilized and its cell-surface expression is decreased.

Cfr can act as a regulator of the TGF $\beta$  signalling pathway, but it needs to be on the cell surface to function as a regulator of the Fgf signalling pathway or a ligand for E-selectin. We also observed that wild-type Cfr expressed in Ba/F3 cells and NIH 3T3 cells occurred not only in the Golgi apparatus, but also on the cell surface (Figures 1B and 8A), and it has been reported that endogenous Cfr is also expressed on the cell surface in 32Dcl3 cells and neutrophils [17]. Therefore we investigated the mechanisms regulating the intracellular distribution of Cfr.

Previous studies have shown that the cytoplasmic tail is important for the localization of Cfr to the Golgi apparatus in

mice and humans [10,11]. We also confirmed that it is required for the retention of Cfr in the Golgi apparatus in mice (Figures 1B and 1C). In addition, we revealed that replacement of the transmembrane and cytoplasmic domains with the GPI anchor signal sequence further enhanced the cell-surface expression (Figures 1B and 1C). From these results, not only the cytoplasmic tail but also the transmembrane domain could contribute to the retention of Cfr in the Golgi apparatus, like many other transmembrane proteins in the Golgi apparatus [18]. Moreover, these C-terminally modified mutants were extremely unstable compared with full-length Cfr, indicating that having left the

Golgi apparatus Cfr is destabilized (Figure 3A). This possibility was further directly confirmed by the protein stability assay. The Cfr mutants that were no longer localized in the Golgi apparatus exhibited much shorter half-lives compared with full-length Cfr (Figure 6). Unexpectedly, this destabilization is not due to the lysosome or proteasome (Figures 3B and 3C). Therefore we searched by mutagenic analysis for regions responsible for the instability.

It has been reported that the extracellular domain of Cfr is cleaved and secreted into the culture supernatant. The molecular mass of the secreted Cfr fragment almost corresponded with that of the extracellular domain, indicating that the cleavage occurs very near the transmembrane domain of Cfr [8,12]. Indeed, we also observed the shed extracellular domain of Cfr in the culture supernatants, but its amount was comparable between FLAG-Cfr and FLAG-Cfr-GPI. These results indicate that the shedding is not a main cause of the instability of Cfr outside the Golgi apparatus. As it was suggested previously that basic amino acid residues in the juxtamembrane region are the targets of the cleavage [8], we examined further the possibility that the cleavage contributes to the instability by making substitutions with an alanine residue. However, the expression of FLAG-Cfr-GPI protein was not affected by the mutations (Figures 4B and 4C). Instead, we found that deletion of the last four Cfr repeats dramatically enhanced the cell-surface expression of FLAG-Cfr-GPI (Figure 5). To find the specific site for the instability, we deleted the last repeat or two repeats from FLAG-Cfr-GPI and found that the surface expression of these GPI-anchored mutants reduced gradually depending on the number of Cfr repeats (Figure 5A). These results suggest that the Cfr repeats rather than a specific sequence for cleavage in the juxtamembrane region are responsible for the instability of Cfr. Interestingly, the repeats also reduced the amount of EpCAM protein when they were inserted in its juxtamembrane region (Figure 8). These results also support that the Cfr repeats function as a general module for protein destabilization.

To examine the function of the Cfr repeat further, we deleted the last four repeats from the full-length Cfr (Figure 1A). However, FLAG-Cfr $\Delta$ 13-16 was still found in the Golgi apparatus, indicating that the presence of the transmembrane domain and cytoplasmic tail is sufficient for the retention of Cfr in the Golgi apparatus (Figures 7A and 7C). Moreover, the stability control via the Cfr repeats does not take place in the Golgi apparatus, because the amount and half-life of FLAG-Cfr $\Delta$ 13-16 were comparable with that of FLAG-Cfr (Figures 6A and 7B). This observation also excludes the possibility that the stability control by the Cfr repeat is due to non-specific effects. These results clearly demonstrate that Cfr is destabilized after passing through the Golgi apparatus.

On the basis of our findings, we propose a two-step model for regulation of the intracellular distribution of Cfr (Figure 8G). First, Cfr is retained via its transmembrane domain and cytoplasmic tail in the Golgi apparatus in a manner similar to that of many other transmembrane proteins. It has been accepted that transmembrane proteins located in the Golgi apparatus have a relatively short transmembrane domain (~15 amino acids) compared with that of the plasma membrane proteins (~20 amino acids). This short transmembrane domain fits the properties of lipids constituting the membrane of the Golgi apparatus and retains proteins with this domain in the Golgi apparatus [19]. However, the transmembrane domain of Cfr is composed of 21 amino acids, indicating that the localization of Cfr in the Golgi apparatus is independent of the length of the transmembrane domain. Furthermore, the tyrosine-based motif in the cytoplasmic domain functions as a retrieval signal from the plasma membrane to the Golgi apparatus in some transmembrane

proteins located in the Golgi apparatus such as TGOLN2 [20-22]. However, Cfr has no tyrosine residues in its cytoplasmic tail, indicating that Cfr occurs in the Golgi apparatus by other mechanisms. It has been reported that the transmembrane domains and cytoplasmic regions interact with each other to form a large complex, preventing transport to other destinations (the 'kin recognition' mechanism) [18,23]. This is a possible mechanism regulating the distribution of Cfr. If Cfr is also retained in the Golgi apparatus by 'kin recognition', modification of the transmembrane region and cytoplasmic tail should alter the intracellular localization of Cfr. Secondly, after leaving the Golgi apparatus, Cfr is destabilized via its Cfr repeats in the juxtamembrane region, resulting in reduced cell-surface expression. This step seems to be specific to Cfr, and we speculate that there may be a factor recognizing the Cfr repeats to destabilize Cfr. The fact that EpCAM-CfrRepeat is also further destabilized supports the existence of a *trans*-acting factor on the Cfr repeats (Figure 8). Therefore expression of this factor, or modification of the recognized sites in the Cfr repeat should affect the localization of Cfr. Alternatively, a portion of Cfr may be transported to the surface by simply escaping from this two-step regulation when expressed abundantly. Thus the intracellular distribution of Cfr can be modified at multiple points to direct it into the Golgi apparatus, or on to the cell surface, determining its functions.

#### AUTHOR CONTRIBUTION

Yuichiro Miyaoka, Hidenori Kato and Kazuki Ebato performed the experiments and analysed the data. Shigeru Saito and Naoko Miyata performed the cell sorting. Toru Imamura contributed the Ba/F3 cell line expressing Fgfr3c and provided advice on experimental design. Yuichiro Miyaoka designed the research project. Yuichiro Miyaoka and Atsushi Miyajima wrote the paper.

#### ACKNOWLEDGEMENTS

We thank Dr M. Asada and Dr M. Suzuki (National Institute of Advanced Industrial Science and Technology, Tsukuba, Japan) for helpful discussions. We also thank Dr D.M. Ornitz (Washington University, St Louis, MO, U.S.A.) and Dr Y. Yamazumi (The University of Tokyo, Tokyo, Japan) for providing cDNA for Fgfrs and human cDNA respectively.

#### FUNDING

This work was supported, in part, by a Grant-in-Aid for Young Scientists [grant number 22791363 (to Y.M.)] and a Grant-in-Aid for Scientific Research to A.M. from the Ministry of Education, Science and Culture, Japan and the Takeda Science Foundation.

#### REFERENCES

- Burrus, L. W. and Olwin, B. B. (1989) Isolation of a receptor for acidic and basic fibroblast growth factor from embryonic chick. *J. Biol. Chem.* **264**, 18647-18653
- Zhou, Z., Zuber, M. E., Burrus, L. W. and Olwin, B. B. (1997) Identification and characterization of a fibroblast growth factor (FGF) binding domain in the cysteine-rich FGF receptor. *J. Biol. Chem.* **272**, 5167-5174
- Miyaoka, Y., Tanaka, M., Imamura, T., Takada, S. and Miyajima, A. (2010) A novel regulatory mechanism for Fgf18 signaling involving cysteine-rich FGF receptor (Cfr) and delta-like protein (Dlk). *Development* **137**, 159-167
- Gonatas, J. O., Meztis, S. G., Stieber, A., Fleischer, B. and Gonatas, N. K. (1989) MG-160. A novel sialoglycoprotein of the medial cisternae of the Golgi apparatus. *J. Biol. Chem.* **264**, 646-653
- Croul, S., Meztis, S. G., Stieber, A., Chen, Y. J., Gonatas, J. O., Goud, B. and Gonatas, N. K. (1990) Immunocytochemical visualization of the Golgi apparatus in several species, including human, and tissues with an antiserum against MG-160, a sialoglycoprotein of rat Golgi apparatus. *J. Histochem. Cytochem.* **38**, 957-963
- Stieber, A., Mourelatos, Z., Chen, Y. J., Le Douarin, N. and Gonatas, N. K. (1995) MG160, a membrane protein of the Golgi apparatus which is homologous to a fibroblast growth factor receptor and to a ligand for E-selectin, is found only in the Golgi apparatus and appears early in chicken embryo development. *Exp. Cell Res.* **219**, 562-570

- 7 Steegmaier, M., Levinovitz, A., Isenmann, S., Borges, E., Lenter, M., Kocher, H. P., Kleuser, B. and Vestweber, D. (1995) The E-selectin-ligand ESL-1 is a variant of a receptor for fibroblast growth factor. *Nature* **373**, 615–620
- 8 Olofsson, A., Hellman, U., Ten Dijke, P., Grimsby, S., Ichijo, H., Moren, A., Miyazono, K. and Heldin, C. H. (1997) Latent transforming growth factor- $\beta$  complex in Chinese hamster ovary cells contains the multifunctional cysteine-rich fibroblast growth factor receptor, also termed E-selectin-ligand or MG-160. *Biochem J.* **324**, 427–434
- 9 Yang, T., Mendoza-Londono, R., Lu, H., Tao, J., Li, K., Keller, B., Jiang, M. M., Shah, R., Chen, Y., Bertin, T. K. et al. (2010) E-selectin ligand-1 regulates growth plate homeostasis in mice by inhibiting the intracellular processing and secretion of mature TGF- $\beta$ . *J. Clin. Invest.* **120**, 2474–2485
- 10 Gonatas, J. O., Chen, Y. J., Stieber, A., Mourelatos, Z. and Gonatas, N. K. (1998) Truncations of the C-terminal cytoplasmic domain of MG160, a medial Golgi sialoglycoprotein, result in its partial transport to the plasma membrane and filopodia. *J. Cell Sci.* **111**, 249–260
- 11 Ahn, J., Febbraio, M. and Silverstein, R. L. (2005) A novel isoform of human Golgi complex-localized glycoprotein-1 (also known as E-selectin ligand-1, MG-160 and cysteine-rich fibroblast growth factor receptor) targets differential subcellular localization. *J. Cell Sci.* **118**, 1725–1731
- 12 Antoine, M., Kohl, R., Tag, C. G., Gressner, A. M., Hellerbrand, C. and Kiefer, P. (2009) Secreted cysteine-rich FGF receptor derives from post-translational processing by furin-like pro-hormone convertases. *Biochem. Biophys. Res. Commun.* **382**, 359–364
- 13 Notohamiprodojo, M., Djafarzadeh, R., Mojaat, A., von Lutichau, I., Grone, H. J. and Nelson, P. J. (2006) Generation of GPI-linked CCL5 based chemokine receptor antagonists for the suppression of acute vascular damage during allograft transplantation. *Protein Eng. Des. Sel.* **19**, 27–35
- 14 Okabe, M., Tsukahara, Y., Tanaka, M., Suzuki, K., Saito, S., Kamiya, Y., Tsujimura, T., Nakamura, K. and Miyajima, A. (2009) Potential hepatic stem cells reside in EpCAM + cells of normal and injured mouse liver. *Development* **136**, 1951–1960
- 15 Miyaoka, Y., Tanaka, M., Naiki, T. and Miyajima, A. (2006) Oncostatin M inhibits adipogenesis through the RAS/ERK and STAT5 signaling pathways. *J. Biol. Chem.* **281**, 37913–37920
- 16 Hidalgo, A., Peired, A. J., Wild, M. K., Vestweber, D. and Frenette, P. S. (2007) Complete identification of E-selectin ligands on neutrophils reveals distinct functions of PSGL-1, ESL-1, and CD44. *Immunity* **26**, 477–489
- 17 Steegmaier, M., Borges, E., Berger, J., Schwarz, H. and Vestweber, D. (1997) The E-selectin-ligand ESL-1 is located in the Golgi as well as on microvilli on the cell surface. *J. Cell Sci.* **110**, 687–694
- 18 Gleeson, P. A. (1998) Targeting of proteins to the Golgi apparatus. *Histochem. Cell Biol.* **109**, 517–532
- 19 Bretscher, M. S. and Munro, S. (1993) Cholesterol and the Golgi apparatus. *Science* **261**, 1280–1281
- 20 Bos, K., Wraight, C. and Stanley, K. K. (1993) TGN38 is maintained in the *trans*-Golgi network by a tyrosine-containing motif in the cytoplasmic domain. *EMBO J.* **12**, 2219–2228
- 21 Humphrey, J. S., Peters, P. J., Yuan, L. C. and Bonifacio, J. S. (1993) Localization of TGN38 to the *trans*-Golgi network: involvement of a cytoplasmic tyrosine-containing sequence. *J. Cell Biol.* **120**, 1123–1135
- 22 Ponnambalam, S., Rabouille, C., Luzio, J. P., Nilsson, T. and Warren, G. (1994) The TGN38 glycoprotein contains two non-overlapping signals that mediate localization to the *trans*-Golgi network. *J. Cell Biol.* **125**, 253–268
- 23 Chen, W. and Stanley, P. (2003) Five Lec1 CHO cell mutants have distinct *Mgat1* gene mutations that encode truncated *N*-acetylglucosaminyltransferase I. *Glycobiology* **13**, 43–50

Received 18 February 2011/11 July 2011; accepted 21 July 2011

Published as BJ Immediate Publication 21 July 2011, doi:10.1042/BJ20110318

**Identification and Isolation of Adult Liver Stem/Progenitor Cells** 2  
3

**Minoru Tanaka and Atsushi Miyajima** 4

**Abstract** 5

Hepatoblasts are considered to be liver stem/progenitor cells in the fetus because they propagate and differentiate into two types of liver epithelial cells, hepatocytes and cholangiocytes. In adults, oval cells that emerge in severely injured liver are considered facultative hepatic stem/progenitor cells. However, the nature of oval cells has remained unclear for some time due to the lack of a method to isolate them. It has also been unclear whether liver stem/progenitor cells exist in normal adult liver. Recently, we and others have successfully identified oval cells and adult liver stem/progenitor cells. Here, we describe the identification and isolation of mouse liver stem/progenitor cells by utilizing antibodies against specific cell surface marker molecules. 6  
7  
8  
9  
10  
11  
12  
13

**Key words:** Liver stem/progenitor cells, Oval cells, Flow cytometry, Antibody 14

---

**1. Introduction** 15

The adult liver has a remarkable potential to regenerate when injured. In many cases, hepatocytes replicate to repair the damage (1, 2). However, if the injury limits the proliferation of hepatocytes, facultative progenitor cells proliferate around portal veins; this is known as a ductal reaction (3, 4). These proliferating epithelial cells, often referred to as “oval cells” in rodents, are believed to contribute to liver regeneration (5). The nature of oval cells as liver stem cells has been debated based on numerous studies using various rodent models. In mice, a diet containing 3,5-diethoxycarbonyl-1,4-dihydro-collidine (DDC) and a choline-deficient, ethionine-supplemented (CDE) diet have been developed to induce oval cell activation (6–8). Although these proliferating epithelial cells upon 16  
17  
18  
19  
20  
21  
22  
23  
24  
25  
26  
27

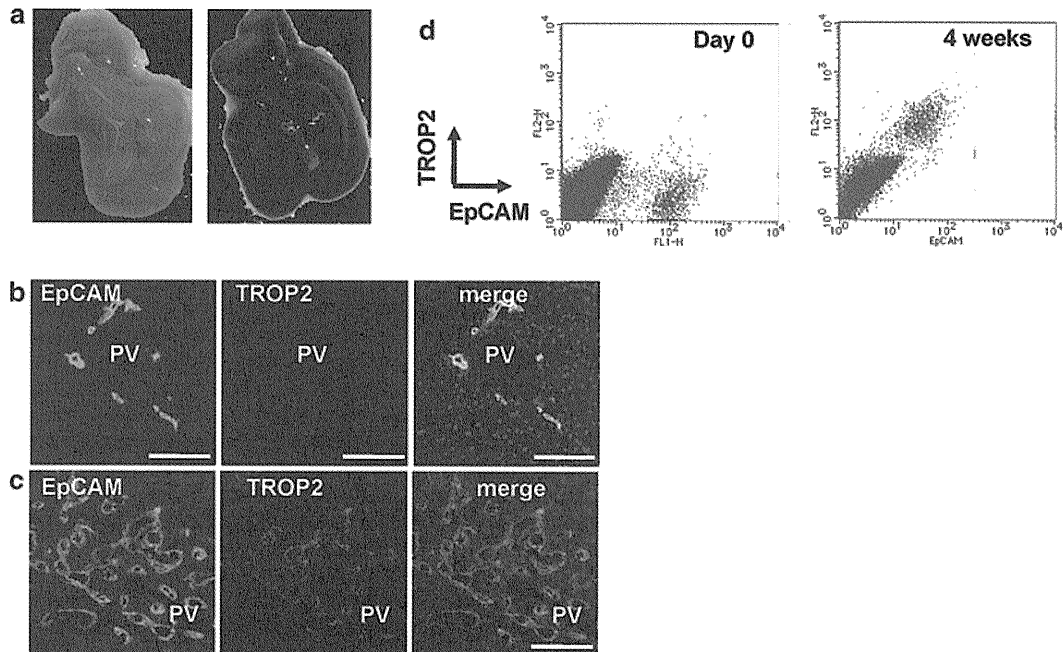


Fig. 1. The DDC-containing diet causes hepatic injury and oval cell activation. (a) Appearance of normal liver (*left panel*) and liver damaged by DDC (*right panel*). (b, c) Immunohistochemistry of frozen sections of normal liver (b) and the liver of mice fed DDC for 5 weeks (c) with anti-EpCAM and anti-TROP2 Abs. TROP2 is expressed in oval cells but not in normal cholangiocytes. (d) Flow cytometric analysis of nonparenchymal cells with anti-EpCAM and anti-TROP2 Abs after DDC feeding. PV portal vein. Scale bar, 100  $\mu$ m.

28  
29  
30  
31  
32  
33  
34  
35  
36  
37  
38  
39  
40

injury by various insults are collectively referred to as oval cells, it remains unclear whether or not those cells in different species by different protocols have common characteristics. To address this issue, oval cells need to be precisely identified and isolated for clonal analysis. Recently, we and others have identified and characterized adult liver stem/progenitor cells by utilizing cell surface markers (9–13). We identified TROP2 and epithelial cell adhesion molecule (EpCAM) as markers expressed in oval cells (Fig. 1) and by using antibodies, isolated the oval cell compartment from the injured livers of mice fed a diet containing DDC. Furthermore, we developed culture system and characterized EpCAM<sup>+</sup> cells isolated from normal as well as injured livers. Here, we describe the methods for identifying and isolating mouse liver stem/progenitor cells.

## 41 2. Materials

### 42 2.1. Generation of Oval 43 Cells in Mouse Liver

44

1. Adult male mice (8–12 weeks old). C57BL/6 mice were used for all experiments.
2. Diet containing 0.1% DDC (Bio-Serv).

3 Identification and Isolation of Adult Liver Stem/Progenitor Cells

**2.2. Immuno-histochemistry of Frozen Liver Sections by Zamboni's Fixation (A Modified Paraformaldehyde-Based Fixation Method)**

1. Solution A: Saturated Picric acid solution in distilled water available commercially from Sigma-Aldrich, etc. Any solid materials were removed by filtration before use. 45  
46  
47
2. Solution B: Twenty grams of paraformaldehyde were dissolved in 100 mL of distilled water. The solution was warmed to 60°C and stirred to melt the paraformaldehyde. A small amount of 1 N NaOH was added if necessary. After complete dissolution, the solution was cooled down. If necessary, it was filtrated. 48  
49  
50  
51  
52
3. Zamboni's solution: 150 mL of solution A and 100 mL of solution B were mixed well, and 750 mL of PBS (pH 7.4) added to adjust the total volume to 1 L. This solution can be stored at 4°C for at least 1 year. 53  
54  
55  
56

**2.3. Isolation of EpCAM+ Cells from Livers of Normal and DDC Diet-Fed Mice**

[AU1]

1. Perfusion solution I: Liver Perfusion Medium (GIBCO 17701-038). 57  
58
2. Perfusion solution II: 8 g NaCl, 0.4 g KCl, 0.56 g CaCl<sub>2</sub>, 0.078 g NaH<sub>2</sub>PO<sub>4</sub>·2H<sub>2</sub>O, 0.151 g Na<sub>2</sub>HPO<sub>4</sub>·12H<sub>2</sub>O, 0.9 g glucose, 0.35 g NaHCO<sub>3</sub>, and 2.38 g HEPES were dissolved in distilled and deionized water [made up to 1 L and filtered through a 0.22-µm STERICUP (Millipore)]. 59  
60  
61  
62  
63
3. Collagenase solution I: 50 mg of collagenase (Sigma C-5138), 25 mg of DNaseI (Sigma DN25-1G), and 10 mL of FBS were added to 90 mL of perfusion solution II, mixed well, and filtered through a 0.22-µm STERICUP (Millipore) (made fresh as required) (see Note 1). 64  
65  
66  
67  
68
4. Collagenase solution II: 50 mg of pronase (Roche) was dissolved in 100 mL of Collagenase solution I, mixed well, and filtered through a 0.22-µm STERICUP (Millipore) (made fresh as required). 69  
70  
71  
72
5. Washing solution: William's E medium containing 10% FBS. 73
6. Hemolysis buffer: 1 g of Trizma base (Sigma) and 2.8 g of NH<sub>4</sub>Cl were dissolved in 500 mL of distilled and deionized water. 74  
75
7. Catheter of 24 G×3/4" indwelling needle (TERUMO, SR-OT2419C). 76  
77
8. Peristaltic pump: Masterflex L/S Variable-Speed Modular Drives (HV-07553-80) with silicone tubing (HV-96410-13) (Cole-Parmer, IL). 78  
79  
80
9. Antibodies: Biotinylated goat anti-TROP2 antibody (BAF1122) (R&D Systems), rat anti-EpCAM antibody (Clone G8.8) (BioLegend) or (Clone 2-17) (MBL International), and FcBlock (BD). 81  
82  
83  
84

**2.4. Culture of EpCAM+ Cells Isolated from Normal and DDC Diet-Fed Liver**

1. Standard medium: Williams' medium E containing 10% FBS, 10 mM nicotinamide, 2 mM L-glutamine, 0.2 mM ascorbic acid, 20 mM HEPES pH 7.5, 1 mM sodium pyruvate, 17.6 mM NaHCO<sub>3</sub>, 14 mM glucose, 100 nM dexamethasone, 85  
86  
87  
88

- 89 1× ITS (insulin, transferrin, selenium X) (GIBCO) and 50 µg/mL  
 90 gentamicin.  
 91 2. Cytokines: Human EGF and human recombinant HGF (final  
 92 concentration of 10 ng/mL each).  
 93 3. Type-I collagen-coated dish: 35 mm dishes were coated with  
 94 Type-I collagen solution (Cellmatrix Type I-C, Nitta gelatin).  
 95 4. Trypsin: 0.25% Trypsin–EDTA (#25200)(GIBCO).

---

96 **3. Methods**

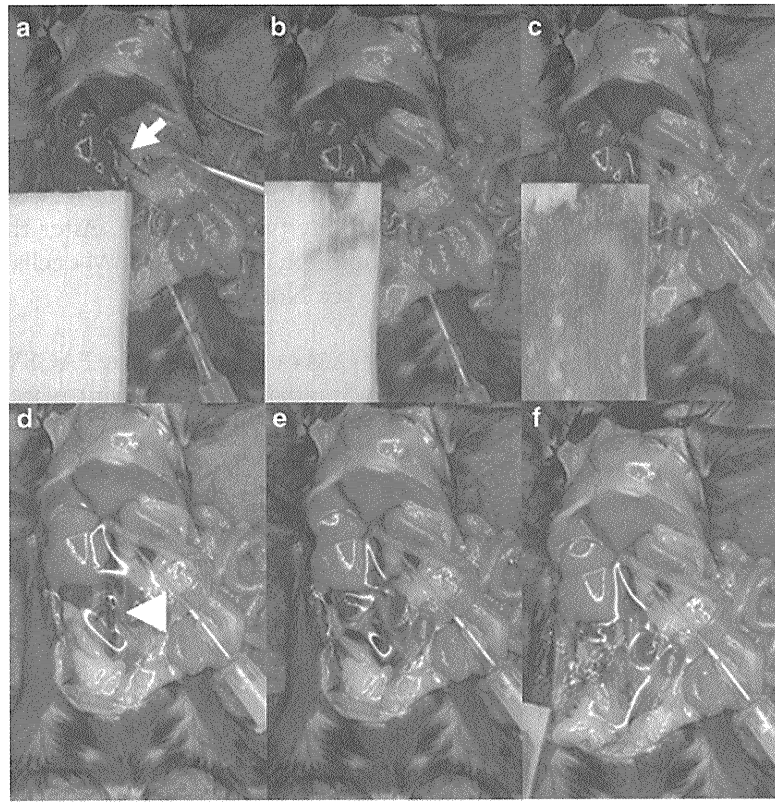
97 **3.1. Generation of Oval**  
 98 **Cells and Immuno-**  
 99 **histochemistry**

- 100 1. Mice were fed by the DDC-containing diet for more than  
 101 4 weeks (see Note 2). After sacrifice, the whole livers were  
 102 removed carefully, dissected into pieces of 5 mm and fixed by  
 103 incubation in Zamboni's solution at 4°C for 8 h to O/N (see  
 104 Note 3).  
 105 2. The fixed tissues were immersed in 10% sucrose/PBS, 15%  
 106 sucrose/PBS, and 20% sucrose/PBS for 1 day each. Then, the  
 107 tissues were frozen in OCT compound. Sections (8 µm) were  
 prepared with a cryostat and incubated with each antibody,  
 followed by a fluorescein-conjugated secondary antibody (see  
 Note 4).

108 **3.2. Isolation**  
 109 **of EpCAM+ Cells**  
 110 **from Mouse Liver**

- 111 1. Liver perfusion solution I (20 mL per a mouse) and colla-  
 112 genase solution I (25 mL per mouse) were warmed at 37°C in a  
 water bath, and a 50-mL glass beaker containing collagenase  
 solution II (10 mL per mouse) was placed in an air incubator  
 at 37°C.  
 113 2. An anesthetized mouse was fixed on a cork board and 70%  
 114 ethanol sprayed on the abdominal skin. The abdomen was  
 115 opened and the intestine moved over to the right side (Fig. 2a).  
 116 The portal vein was cut with surgical scissors without broken  
 117 away. The bleeding was absorbed with cotton gauze to prevent  
 118 blood from pooling (Fig. 2b). The hole was cannulated with a  
 119 catheter connected to a peristaltic pump (Fig. 2c) (see Note  
 120 5). Perfusion solution I was delivered at a speed of 3 mL/min  
 121 (Fig. 2d) and then the vena cava inferior was cut (Fig. 2e).  
 122 After perfusion for 5 min (total volume, approximately 15 mL)  
 123 (Fig. 2f), perfusion solution I was replaced with collagenase  
 124 solution I and the perfusion continued for 8 min (total volume,  
 125 approximately 25 mL).  
 126 3. After digestion, the whole liver was carefully removed and  
 127 transferred to a Petri dish (10 cm in diameter) (see Note 6).  
 128 20 mL of washing solution was added to the dish and the  
 129 liver capsule was torn by crossing two pairs of fine tweezers.

3 Identification and Isolation of Adult Liver Stem/Progenitor Cells



Arrow; portal vein, arrowhead; vena cava

[AU2]

Fig.-2- Gannulation of mouse liver.

The contents of the liver were dispersed in the solution and pipetted up and down actively until no lumps remained (see Note 7). Then, the cell suspension was passed through a 70- $\mu\text{m}$  filter to remove undigested clots, including the biliary tree and the filtrate was kept on ice (Cell Suspension A). The residual mass on the filter was transferred to prewarmed collagenase solution II and stirred on a magnetic stirrer for 20 min at 37°C in an air incubator. After digestion, it was pipetted up and down and filtered as previously explained (Cell Suspension B).

4. Cell Suspension A and Cell Suspension B were mixed in a 50 mL disposable tube and washing solution was added to make a total volume of 50 mL. The solution was centrifuged at approximately 100 $\times g$  for 2 min to remove parenchymal cells (hepatocytes). The supernatant was transferred to another fresh tube and the centrifugation was repeated twice.
5. After centrifugation of the supernatant at 300 $\times g$  for 5 min, the pellet was suspended with 7 mL of hemolysis buffer and kept on ice for 3 min. Then, 8 mL of washing solution was added and centrifuged at 300 $\times g$  for 5 min. The pellet was resuspended



149  
150  
151  
152  
153  
154  
155  
156  
157

with 10 mL of 3% FBS/PBS and filtered with 70  $\mu$ m mesh to remove debris (see Note 9).

6. After centrifugation at  $300\times g$  for 5 min, the pellet was resuspended in 300–500  $\mu$ L of 3% FBS/PBS. Nonspecific binding was blocked by incubating with FcBlock, and the cell suspension was incubated with fluorescein-conjugated anti-EpCAM antibody (see Note 10). After the staining of dead cells with propidium iodide, EpCAM+ cells were sorted by FACSVantage SE (see Note 11).

158 **3.3. Culture of**  
159 **EpCAM+ Cells Isolated**  
160 **from Normal and DDC**  
161 **Diet-Fed Liver**  
162

1. EpCAM+ cells isolated by FACSVantage SE were suspended in the Standard Medium and plated at  $1\times 10^4$  cells per Type-I collagen-coated 35-mm dish. Human EGF and human recombinant HGF were added to the culture to a final concentration of 10 ng/mL each.

2. After 9 days of culture, the proliferating cells were trypsinized, washed, and replated onto new culture dishes (Fig. 3) (see Note 12). They continued to grow even after serial passages for more than 6 months, and possessed the potential to differentiate into hepatocytic and cholangiocytic cell lineages under the adequate culture conditions (12).

163  
164  
165  
166  
167  
168

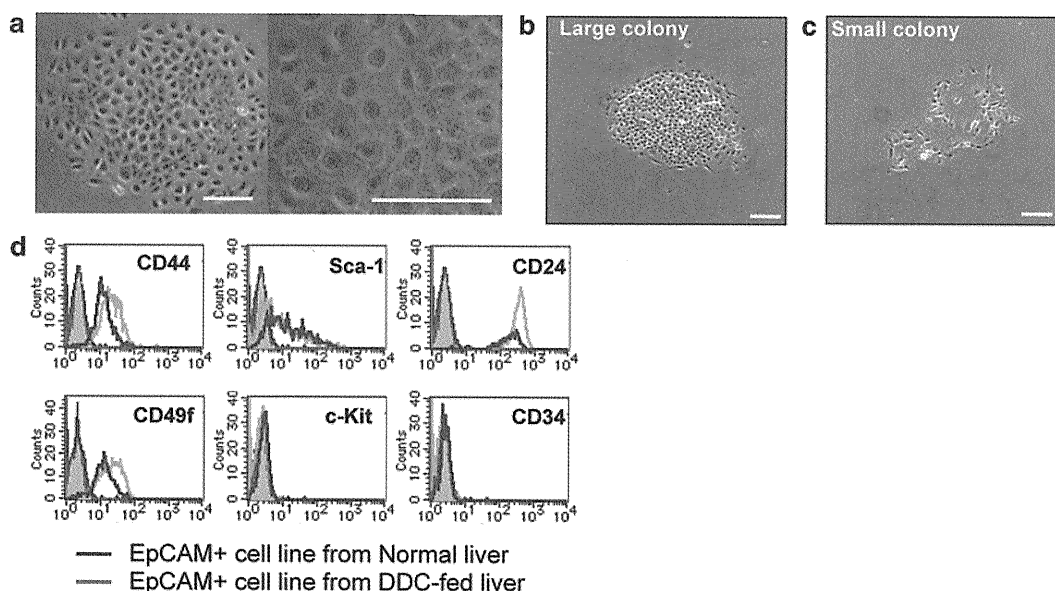


Fig. 3. Characteristics of proliferative EpCAM+ cells. (a) Morphology of proliferative cells with characteristic of liver stem cells derived from EpCAM+ cells of DDC diet-fed livers. (b, c) Appearance of a large colony (b) with the potential to proliferate, and a small colony (c) with limited growth derived from EpCAM+ cells of normal livers. (d) Flow cytometric analysis of some cell surface markers in established cell lines with characteristics of liver stem cells. The cells derived from normal (blue line) and DDC diet-fed (red line) livers show similar expression profiles of cell surface markers. Scale bar: 200  $\mu$ m.

**4. Notes**

169

1. Chronic hepatitis induced by the administration of DDC often makes the liver fibrotic. We recommend this collagenase for efficient digestion of the fibrotic liver. Aliquots of collagenase powder were stored at  $-80^{\circ}\text{C}$  until used. Avoid freezing and thawing to maintain the enzymatic activity. 170-174
2. The formation of oval cells reaches a plateau at about 4 weeks after the administration of DDC. Prolonged administration for more than 8 weeks may cause death. 175-177
3. We strongly recommend Zamboni's solution for the detection of TROP2 because the signal is very faint with other reagents, such as 4% PFA and cold acetone. 178-180
4. We usually incubated frozen sections with the first antibody solution (1/50–100 dilution with 5% skim milk/PBS) at  $4^{\circ}\text{C}$  for O/N. We used goat anti-TROP2 antibody (BAF1122) (R&D Systems) and rat anti-EpCAM antibody (Clone G8.8) for immunostaining. 181-185
5. We usually cannulated with running solution at a very low speed. Put the catheter toward the bleeding portal vein. Do not insert the catheter too deep into the liver or you will damage a vein. If the perfusion is successfully performed, the liver turns yellowish due to blood removal as shown in Fig. 2d. 186-190
6. We usually removed the gall bladder carefully without burst because the bile is toxic. 191-192
7. We prefer to use a glass pipette with a latex nipple. This permits vigorous pipetting to disperse the clump of tissues rather than electrical pipettes. 193-195
8. Repeat this step until the cell pellet is completely dissolved. 196
9. Insoluble debris should be removed by filtration to proceed to the flow cytometric analysis. 197-198
10. We usually use FITC-conjugated rat anti-EpCAM antibody (Clone 2–17). 199-200
11. We recommend a magnetic bead-based cell separation system to enrich EpCAM+ cells before purification by flow cytometry. We usually use the autoMACS system with anti-FITC microbeads before cell sorting by FACSVantage, which saves time for cell sorting and avoids reducing the viability of EpCAM+ cells. 201-206
12. The primary culture contains both small and large colonies at this point. The proliferative cells with characteristics of liver stem/progenitor cells are selectively expanded by serial passages. 207-210

## 211 References

- 248 1. Michalopoulos, G. K. (2010) Liver regeneration  
249 after partial hepatectomy: critical analysis of  
247 mechanistic dilemmas. *Am J Pathol* **176**,  
245 2–13.
- 249 2. Overturf, K., al-Dhalimy, M., Ou, C. N.,  
250 Finegold, M. and Grompe, M. (1997) Serial  
258 transplantation reveals the stem-cell-like regenerative  
259 potential of adult mouse hepatocytes.  
259 *Am J Pathol* **151**, 1273–1280.
- 284 3. Alison, M. R., Golding, M., Sarraf, C. E.,  
285 Edwards, R. J. and Lalani, E. N. (1996) Liver  
286 damage in the rat induces hepatocyte stem cells  
287 from biliary epithelial cells. *Gastroenterology*  
285 **110**, 1182–1190.
- 289 4. Theise, N. D., Saxena, R., Portmann, B. C.,  
290 Thung, S. N., Yee, H., Chiriboga, L., et al.  
288 (1999) The canals of Hering and hepatic stem  
289 cells in humans. *Hepatology* **30**, 1425–1433.
- 290 5. Farber, E. (1956) Similarities in the sequence  
294 of early histological changes induced in the  
293 liver of the rat by ethionine, 2-acetylaminofluorene,  
296 and 3'-methyl-4-dimethylaminobenzene. *Cancer Res* **16**, 142–148.
- 296 6. Akhurst, B., Croager, E. J., Farley-Roche, C.  
299 A., Ong, J. K., Dumble, M. L., Knight, B.,  
297 et al. (2001) A modified choline-deficient,  
298 ethionine-supplemented diet protocol effectively  
299 induces oval cells in mouse liver.  
299 *Hepatology* **34**, 519–522.
- 274 7. Preisegger, K. H., Factor, V. M., Fuchsichler,  
275 A., Stumptner, C., Denk, H. and Thorgeirsson,  
276 S. S. (1999) Atypical ductular proliferation and  
277 its inhibition by transforming growth factor  
beta1 in the 3,5-diethoxycarbonyl-1,4-dihydrocollidine mouse model for chronic alcoholic liver disease. *Lab Invest* **79**, 103–109.
8. Wang, X., Foster, M., Al-Dhalimy, M., Lagasse, E., Finegold, M. and Grompe, M. (2003) The origin and liver repopulating capacity of murine oval cells. *Proc Natl Acad Sci U S A* **100** Suppl 1, 11881–11888.
9. Schmelzer, E., Zhang, L., Bruce, A., Wauthier, E., Ludlow, J., Yao, H. L., et al. (2007) Human hepatic stem cells from fetal and postnatal donors. *J Exp Med* **204**, 1973–1987.
10. Yovchev, M. I., Grozdanov, P. N., Zhou, H., Racherla, H., Guha, C. and Dabeva, M. D. (2008) Identification of adult hepatic progenitor cells capable of repopulating injured rat liver. *Hepatology* **47**, 636–647.
11. Suzuki, A., Sekiya, S., Onishi, M., Oshima, N., Kiyonari, H., Nakauchi, H., et al. (2008) Flow cytometric isolation and clonal identification of self-renewing bipotent hepatic progenitor cells in adult mouse liver. *Hepatology* **48**, 1964–1978.
12. Okabe, M., Tsukahara, Y., Tanaka, M., Suzuki, K., Saito, S., Kamiya, Y., et al. (2009) Potential hepatic stem cells reside in EpCAM+ cells of normal and injured mouse liver. *Development* **136**, 1951–1960.
13. Kamiya, A., Kakinuma, S., Yamazaki, Y. and Nakauchi, H. (2009) Enrichment and clonal culture of progenitor cells during mouse postnatal liver development in mice. *Gastroenterology* **137**, 1114–1126, 1126 e1–14.

# TROP2 Expressed in the Trunk of the Ureteric Duct Regulates Branching Morphogenesis during Kidney Development

Yuko Tsukahara, Minoru Tanaka\*, Atsushi Miyajima\*

Institute of Molecular and Cellular Biosciences, The University of Tokyo, Tokyo, Japan

## Abstract

TROP2, a cell surface protein structurally related to EpCAM, is expressed in various carcinomas, though its function remains largely unknown. We examined the expression of TROP2 and EpCAM in fetal mouse tissues, and found distinct patterns in the ureteric bud of the fetal kidney, which forms a tree-like structure. The tip cells in the ureteric bud proliferate to form branches, whereas the trunk cells differentiate to form a polarized ductal structure. EpCAM was expressed throughout the ureteric bud, whereas TROP2 expression was strongest at the trunk but diminished towards the tips, indicating the distinct cell populations in the ureteric bud. The cells highly expressing TROP2 (TROP2<sup>high</sup>) were negative for Ki67, a proliferating cell marker, and TROP2 and collagen-I were co-localized to the basal membrane of the trunk cells. TROP2<sup>high</sup> cells isolated from the fetal kidney failed to attach and spread on collagen-coated plates. Using MDCK cells, a well-established model for studying the branching morphogenesis of the ureteric bud, TROP2 was shown to inhibit cell spreading and motility on collagen-coated plates, and also branching in collagen-gel cultures, which mimic the ureteric bud's microenvironment. These results together suggest that TROP2 modulates the interaction between the cells and matrix and regulates the formation of the ureteric duct by suppressing branching from the trunk during kidney development.

**Citation:** Tsukahara Y, Tanaka M, Miyajima A (2011) TROP2 Expressed in the Trunk of the Ureteric Duct Regulates Branching Morphogenesis during Kidney Development. *PLoS ONE* 6(12): e28607. doi:10.1371/journal.pone.0028607

**Editor:** Tsutomu Kume, Feinberg Cardiovascular Research Institute, Northwestern University, United States of America

**Received:** August 1, 2011; **Accepted:** November 11, 2011; **Published:** December 14, 2011

**Copyright:** © 2011 Tsukahara et al. This is an open-access article distributed under the terms of the Creative Commons Attribution License, which permits unrestricted use, distribution, and reproduction in any medium, provided the original author and source are credited.

**Funding:** This work was supported by research grants from the Ministry of Education, Culture, Sports, Science and Technology of Japan, Ministry of Health, Labour and Welfare of Japan, the Core Research for Evolutional Science and Technology (CREST) program from the Japan Science and Technology Agency and Takeda Science Foundation. The funders had no role in study design, data collection and analysis, decision to publish, or preparation of the manuscript.

**Competing Interests:** The authors have declared that no competing interests exist.

\* E-mail: tanaka@iam.u-tokyo.ac.jp (MT); miyajima@iam.u-tokyo.ac.jp (AM)

## Introduction

TROP2, also known as EGP-1, M1S1, GA733-1, and TACSTD2, is a 36-kDa membrane glycoprotein, initially identified as a tumor-associated calcium signal transducer (TACSTD) expressed in gastrointestinal, bladder, lung, and cervix carcinomas and later found to be highly expressed in many other tumors including pancreatic cancers and squamous cell carcinomas of the oral cavity [1]. TROP2 is strongly expressed in trophoblasts forming the outer layer of the blastocyst which develops into the placenta [2]. In the prostate, TROP2 is specifically expressed in prostate stem cells located in the basal region [3]. We have recently found that TROP2 is expressed in hepatic progenitor cells known as oval cells, which are produced in response to severe liver injury and form duct-like structures surrounding the portal vein [4].

TROP2 is structurally related to epithelial cell adhesion molecule (EpCAM), also known as TACSTD1. Both TROP2 and EpCAM are type I transmembrane proteins, consisting of a hydrophobic leader peptide, a thyroglobulin-like domain, a single transmembrane domain and a short cytoplasmic domain. The cytoplasmic tail of TROP2, but not EpCAM, contains a region homologous to phosphatidylinositol 4,5-bisphosphate (PIP<sub>2</sub>)-binding motif [5]. EpCAM is widely expressed in epithelial cells and plays roles in cell-cell adhesion, cell proliferation and cell motility [6–10]. On the other hand, TROP2 was suggested to enhance the proliferation of tumor cells in an anchorage-independent manner

[11] and the formation of tight junctions by interacting with Claudin-1 and -7 in the corneal epithelium [12]. However, TROP2 expression in normal tissues and its functions still remain largely unstudied.

In the development of the mammalian kidney, the ureteric bud epithelium proliferates and branches to form a tree-like structure [13,14]. This process is known as branching morphogenesis and depends on interactions of the ureteric bud with the metanephric mesenchyme and also components of the extracellular matrix (ECM). Factors secreted from the metanephric mesenchyme enhance the proliferation, elongation and branching of the ureteric bud cells, resulting in differentiation to form the collecting duct system. On the other hand, ECM components around the ureteric bud modulate growth factor signaling and provide an anchorage for cell migration via the ECM-specific integrin receptors on the ureteric bud cells [15,16].

The cells forming the tip and trunk of the ureteric bud exhibit different characteristics [17]. The tip cells are proliferating immature cells that are located at the branching points and interact with the metanephric mesenchyme. By contrast, the trunk cells are differentiating into the collecting duct with a rigid structure consisting of polarized epithelial cells. While the molecular mechanisms underlying the establishment of the tip structure have been well studied, little is known about the mechanisms of trunk morphogenesis. In particular, the factors